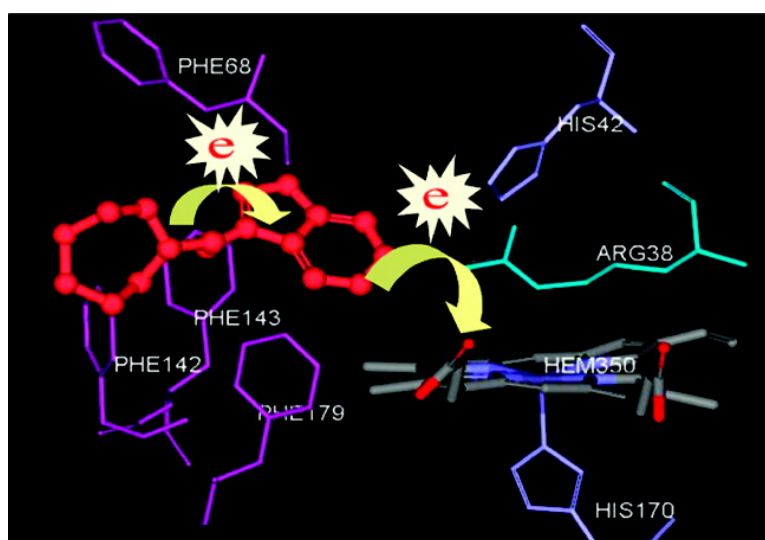**Article**

Oxidations of *N*-(3-Indoleethyl) Cyclic Aliphatic Amines by Horseradish Peroxidase: The Indole Ring Binds to the Enzyme and Mediates Electron-Transfer Amine Oxidation

Ke-Qing Ling, Wen-Shan Li, and Lawrence M. Sayre

More About This Article

Additional resources and features associated with this article are available within the HTML version:

- Supporting Information
- Access to high resolution figures
- Links to articles and content related to this article
- Copyright permission to reproduce figures and/or text from this article

View the Full Text HTML

Oxidations of *N*-(3-Indoleethyl) Cyclic Aliphatic Amines by Horseradish Peroxidase: The Indole Ring Binds to the Enzyme and Mediates Electron-Transfer Amine Oxidation

Ke-Qing Ling,* Wen-Shan Li,[†] and Lawrence M. Sayre*

Department of Chemistry, Case Western Reserve University, Cleveland, Ohio 44106

Received August 6, 2007; E-mail: kxl56@case.edu; lms3@case.edu

Abstract: Although oxidations of aromatic amines by horseradish peroxidase (HRP) are well-known, typical aliphatic amines are not substrates of HRP. In this study, the reactions of *N*-benzyl and *N*-methyl cyclic amines with HRP were found to be slow, but reactions of *N*-(3-indoleethyl) cyclic amines were 2−3 orders of magnitude faster. Analyses of pH-rate profiles revealed a dominant contribution to reaction by the amine-free base forms, the only species found to bind to the enzyme. A metabolic study on a family of congeneric *N*-(3-indoleethyl) cyclic amines indicated competition between amine and indole oxidation pathways. Amine oxidation dominated for the seven- and eight-membered azacycles, where ring size supports the change in hybridization from sp³ to sp² that occurs upon one-electron amine nitrogen oxidation, whereas only indole oxidation was observed for the six-membered ring congener. Optical difference spectroscopic binding data and computational docking simulations suggest that all the arylalkylamine substrates bind to the enzyme through their aromatic termini with similar binding modes and binding affinities. Kinetic saturation was observed for a particularly soluble substrate, consistent with an obligatory role of an enzyme−substrate complexation preceding electron transfer. The significant rate enhancements seen for the indoleethylamine substrates suggest the ability of the bound indole ring to mediate what amounts to medium long-range electron-transfer oxidation of the tertiary amine center by the HRP oxidants. This is the first systematic investigation to document aliphatic amine oxidation by HRP at rates consistent with normal metabolic turnover, and the demonstration that this is facilitated by an auxiliary electron-rich aromatic ring.

Introduction

Recent computational, structural, and spectroscopic studies are revealing details of the factors which control reactivity properties of heme enzymes of the cytochrome P450 and peroxidase superfamilies.[1] In contrast to those P450 enzymes that catalyze oxygen-transfer, electron-transfer, or H-atom transfer mechanisms,[2] oxidations by horseradish peroxidase (HRP) uniformly involve electron-transfer, and its substrates are most frequently electron-rich aromatics.[3] HRP and other peroxidases utilize H_2O_2 (or ROOH) to produce the two-electron oxidized species compound I, usually depicted as a Fe(IV)=O porphyrin radical cation (abbreviated $P^+ \cdot Fe(IV)=O$). Although this is the same active oxidant generated in cytochrome P450 (usually from O_2 and two-electron reduction), HRP is usually considered incapable of either O-transfer or H· abstraction chemistry on account of the inaccessibility of substrates to the "buried" iron center.[4] Reduction of compound I by 1e gives compound II, PFe(IV)=O, which in turn is reduced by 1e to the Fe(III) resting state of the enzyme.[5] Although compound I appears to be more reactive than compound II,[4] the redox potentials have been estimated to be quite similar,[6] and observed differences may be due to the different nature of the two oxidants (the porphyrin highest occupied molecular orbital (HOMO) "hole" for compound I and the Fe(IV) for compound II).

On the basis that at least some amines are oxidized by P450 by electron transfer, as modeled by electrochemical oxidations

[†] Current address: Institute of Chemistry, Academia Sinica, 128 Academia Road Sec. 2, Nankang Taipei 115 Taiwan, Republic of China.

(1) (a) Hersleth, H. P.; Ryde, U.; Rydberg, P.; Gorbitz, C. H.; Andersson, K. K. *J. Inorg. Biochem.* **2006**, *100*, 460−76. (b) Behan, R. K.; Hoffart, L. M.; Stone, K. L.; Krebs, C.; Green, M. T. *J. Am. Chem. Soc.* **2006**, *128*, 11471−4. (c) Harvey, J. N.; Bathelt, C. M.; Mulholland, A. J. *J. Comput. Chem.* **2006**, *27*, 1352−62. (d) Green, M. T.; Dawson, J. H.; Gray, H. B. *Science* **2004**, *304*, 1653−6.

(2) For recent reviews on the mechanisms of cytochrome P450 oxidations, see: (a) Isin, E. M.; Guengerich, F. P. *Biochim. Biophys. Acta* **2007**, *1770*, 314−29. (b) Meunier, B.; de Visser, S. P.; Shaik, S. *Chem. Rev.* **2004**, *104*, 3947−80. (c) Makris, T. M.; Davydov, R.; Denisov, I. G.; Hoffman, B. M.; Sligar, S. G. *Drug Metab. Rev.* **2002**, *34*, 691−708. For recent reports on cytochrome P450 catalyzed amine oxidations, see: (d) Cerny, M. A.; Hanzlik, R. P. *J. Am. Chem. Soc.* **2006**, *128*, 3346−54. (e) Jurva, U.; Bissel, P.; Isin, E. M.; Igarashi, K.; Kuttab, S.; Castagnoli, N., Jr. *J. Am. Chem. Soc.* **2005**, *127*, 12368−77. (f) Shaffer, C. L.; Harriman, S.; Koen, Y. M.; Hanzlik, R. P. *J. Am. Chem. Soc.* **2002**, *124*, 8268−74.

(3) (a) Griffin, B. W.; Davis, D. K.; Bruno, G. V. *Bioorg. Chem.* **1981**, *10*, 342−55. (b) Van, der Zee, J.; Duling, D. R.; Mason, R. P.; Eling, T. E. *J. Biol. Chem.* **1989**, *264*, 19828−36. (c) Shaffer, C. L.; Morton, M. D.; Hanzlik, R. P. *J. Am. Chem. Soc.* **2001**, *123*, 8502−8. (d) Shaffer, C. L.; Morton, M. D.; Hanzlik, R. P. *J. Am. Chem. Soc.* **2001**, *123*, 349−50.

(4) (a) Ator, M. A.; Ortiz de Montellano, P. R.; *J. Biol. Chem.* **1987**, *262*, 1542−51. (b) Ortiz de Montellano, P. R.; *Annu. Rev. Pharmacol. Toxicol.* **1992**, *32*, 89−107.

(5) (a) Dunford, H. B. In *Peroxidases in Chemistry and Biology*; Everse, J., Everse, K. E., Grisham, M. B., Eds.; CRC Press: Boca Raton, FL, 1991; Vol. 2, pp 1−24. (b) Dunford, H. B. *Heme Peroxidases*; John Wiley & Sons, Inc.: New York, 1999.

(6) Hayashi, Y.; Yamazaki, I. *J. Biol. Chem.* **1979**, *254*, 9101−6.

Scheme 1
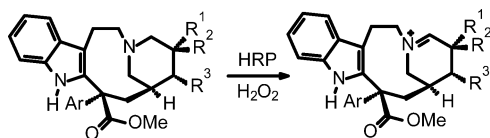
of amines,[7] there has been interest in the plant enzyme HRP as a relatively pure electron-transfer heme oxidant to learn about one-electron oxidation mechanisms important in mammalian metabolism. In this regard, a central question has been why *aliphatic* amines appear to be unreactive toward HRP. One consideration is that only amine "free bases" are subject to oxidation and that typical aliphatic amines are protonated at physiological pH. Thus, whereas a favorable K_d for binding of free base amine to P450 can offset an unfavorable pK_a equilibrium, HRP is known to lack a "normal" substrate binding domain and is thus limited to electron-transfer oxidation of its typical aromatic donor substrates through their fairly weak 1:1 complex association at the "heme crevice."[4,8] Therefore, if HRP is limited to oxidizing those aliphatic amines which have sufficiently low pK_a values to exist at least partly in the free base form in solution at physiological pH, it must then be recognized that structural factors that lower pK_a at the same time increase redox potential. Examples are the typical amine-based "biological buffers" HEPES, PIPES, and MES, which have pK_a values near 7 but are not oxidized by HRP under turnover conditions.[9] Thus, the non-oxidation of aliphatic amines by HRP may reflect the fact that amines with a sufficiently low pK_a have a redox potential too high for the "reach" of HRP.[10,11]

According to this $pK_a-E°$ dichotomy, the optimal amines to test as candidate substrates would be those whose structures confer a low redox potential without raising pK_a. Examples would be azacycles with five-, seven-, and eight-, but not six-membered rings, where the geometry favors the transformation of tetrahedral sp^3 nitrogen to sp^2 trigonal nitrogen that occurs upon 1e oxidation to the aminium radical,[12] but where basicity is essentially constant. However, a preliminary study showed that simple azacycles fail as turnover substrates of HRP.[13] Nonetheless, on the basis that HRP can at least stoichiometrically oxidize the tertiary amine center in certain indole (Vinca) alkaloids to the corresponding iminium species (Scheme 1),[14] we considered the possibility that aliphatic amine oxidation may be facilitated in these molecules by interaction of the indole ring with the usual aryl ring binding domain of HRP.

To test this hypothesis, we synthesized a series of cyclic 3-indoleethylamines **1**−**4** bearing the key *tryptamine* fragment

of the Vinca alkaloid and studied their reactions with HRP compounds I and II in comparison with the corresponding cyclic benzylamines **5**−**8**. Indoles **9** and **10** were included as possible
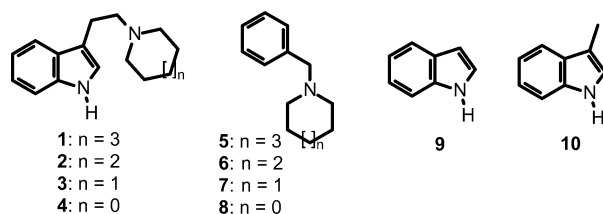
"controls" for the reactions of **1**−**4**. Our results show that the indole ring significantly enhances the HRP-mediated oxidation of aliphatic amine centers with a favorable $pK_a-E°$ balance, and we suggest that this reflects the action of the indole ring not only in promoting binding to the HRP "heme crevice" but also in mediating the electron-transfer oxidation of the amine nitrogen. To our knowledge, this outcome is the first fulfillment of the criteria needed for observation of aliphatic amine oxidation by HRP at rates consistent with normal metabolic turnover.

Results

Kinetics. Reductions of HRP compounds I and II by a given substrate (**1**−**10**) were studied separately in aqueous buffer by monitoring spectrophotometrically the formation of the corresponding enzyme products, compound II and native HRP, respectively, as described previously.[15] Since no turnover was involved, the reaction can be illustrated as

$$E + S \underset{}{\overset{K_d^{app}}{\rightleftharpoons}} ES \xrightarrow{k_{cat}} E' + product$$
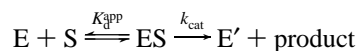
where E represents HRP compound I or compound II, E′ represents HRP compound II or native HRP, and ES represents the enzyme substrate complex. The rate expression can be deduced as

$$rate = \frac{k_{cat}}{K_d^{app} + [S]}[E_0][S] \tag{1}$$

where $[E_0]$ represents the total concentration of free and substrate-bound HRP compound I or compound II, [S] is the substrate concentration, k_{cat} and K_d^{app} are the decomposition rate constant and the apparent dissociation constant of the substrate enzyme complex. Using an excess of substrate with respect to the enzyme, the reaction can be treated according to pseudo-first-order kinetics

$$rate = k_{obsd}[E_0] \tag{2}$$

and the expression of observed rate constant is

$$k_{obsd} = \frac{k_{cat}[S]}{K_d^{app} + [S]} \tag{3}$$

Due to limited solubility of **1**−**10** in aqueous buffer, all the kinetic studies were conducted using micromolar level of substrates. Examples of pseudo-first-order plots are given in Figures 1 and 2. The dependence of k_{obsd} on substrate concen-

(7) (a) Sasaki, J. C.; Fellers, R. S.; Colvin, M. E. *Mutat. Res.* **2002**, *506*−*507*, 79−89. (b) Guengerich, F. P.; Yun, C. H.; Macdonald, T. L. *J. Biol. Chem.* **1996**, *271*, 27321−9.

(8) (a) Fidy, J.; Paul, K.-G.; Vanderkooi, J. M. *Biochemistry* **1989**, *28*, 7531−41. (b) Sukurada, J.; Takahashi, S.; Hosoya, T. *J. Biol. Chem.* **1986**, *261*, 9657−62.

(9) Sayre, L. M.; Naismith, R. T., II; Bada, M. A.; Li, W.-S.; Klein, M. E.; Tennant, M. D. *Biochim. Biophys. Acta* **1996**, *1296*, 250−56.

(10) Guengerich, P.; MacDonald, T. L. *FASEB J.* **1990**, *4*, 2453−9.

(11) Wood, P. M. *Biochem. Soc. Trans.* **1992**, *20*, 349−52.

(12) (a) Lindsay Smith, J. R.; Mead, L. A. V. *J. Chem. Soc., Perkin Trans. 2* **1973**, 206−10. (b) Lindsay Smith, J. R.; Masheder, D. *J. Chem. Soc., Perkin Trans. 2* **1976**, 47−51. (c) Lindsay Smith, J. R.; Masheder, D. *J. Chem. Soc., Perkin Trans. 2* **1977**, 1732−6.

(13) Li, W.-S. Ph.D. Thesis, Case Western Reserve University, Cleveland, OH, 1997.

(14) (a) Elmarakby, S. A.; Duffel, M. W.; Goswami, A.; Sariaslani, F. S.; Rosazza, J. P. N. *J. Med. Chem.* **1989**, *32*, 674−9. (b) Goswami, A.; Macdonald, T. L.; Hubbard, C.; Duffel, M. W.; Rosazza, J. P. N. *Chem. Res. Toxicol.* **1988**, *1*, 238−42.

(15) Ling, K.-Q.; Sayre, L. M. *Bioorg. Med. Chem.* **2005**, *13*, 3543−51.
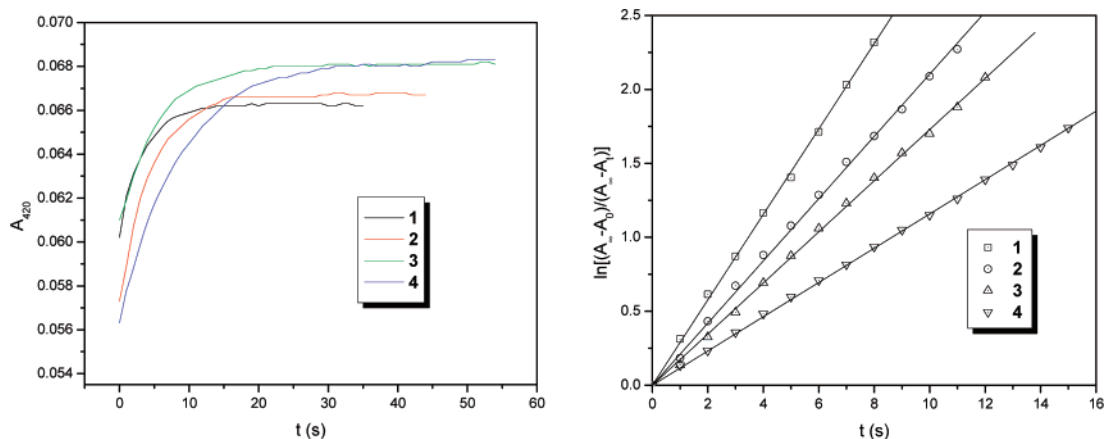
Figure 1. Left panel: time-dependent ΔA_{420} (compound II) recorded during reactions of compound I with **1–4** in 0.1 M pH 9 borate buffer at 25 °C. Right panel: pseudo-first-order $\ln[(A_\infty - A_0)/(A_\infty - A_t)]$ vs t plots. [HRP] = 0.7 μM; [H_2O_2] = 7μM; [**1**], [**2**], [**3**], and [**4**] = 3.5, 14, 28, and 28 μM, respectively.
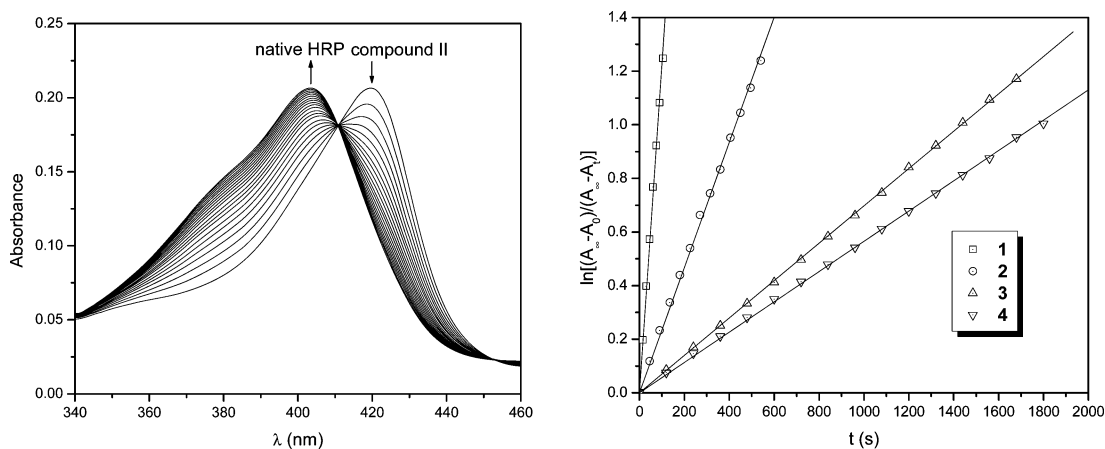

Figure 2. Left panel: time-dependent UV–vis spectra recorded during reaction of compound II with **2** in 0.1 M pH 9 borate buffer at 25 °C (time interval 45 s). Right panel: pseudo-first-order $\ln[(A_\infty - A_0)/(A_\infty - A_t)]$ vs t plots for compound II oxidations of **1–4**. [HRP] = 2.1 μM; [H_2O_2] = 2.1μM; [**1–4**] = 21 μM.

tration in the micromolar range was examined with selected organic substrates at different pH values. Consistent with the millimolar K_d^{app} of these substrates with HRP as shown below, no saturation behavior was observed under these conditions (an example is given in Figure S2). Thus, eq 3 can be simplified as
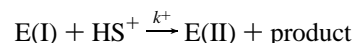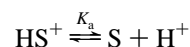
$$k_{obsd} = \frac{k_{cat}}{K_d^{app}} [S] = k_{app}[S] \qquad (4)$$

where k_{app} is the apparent second-order rate constant. Therefore, the k_{app} of each reaction can be extracted directly from k_{obsd} according to eq 4.

   pH-Rate Profiles. The pH dependence of the apparent second-order rate constants (k_{app}) was examined for all the substrates in the range of pH 8–10 to obtain real second-order rate constants independent of the various ionization events in the enzyme and in substrates. The limited pH range studied was because at pH < 8, the rates for most amine substrates were too slow to be measured accurately, whereas at pH > 10, the enzyme became exceedingly unstable.

   Consistent with the lack of ionization for compound I in the range of pH 8–10,[16] the apparent second-order rate constants

(16) Ralston, I.; Dunford, H. B. *Can. J. Biochem.* **1978**, *56*, 1115–9.

for reduction of compound I by indole **9** remained constant (data not shown), and the mean is calculated as the real second-order rate constant (Table 1). For amine substrates, however, the amine ionization plays a role in the net reaction, and one must consider the possible reactions of compound I with both conjugate acid and base:

$$HS^+ \underset{}{\overset{K_a}{\rightleftharpoons}} S + H^+$$

$$E(I) + S \overset{k}{\rightarrow} E(II) + product$$

$$E(I) + HS^+ \overset{k^+}{\longrightarrow} E(II) + product$$

The kinetic expression of the apparent second-order rate constant is deduced as

$$k_{app} = \frac{k}{1 + \dfrac{[H^+]}{K_{app}}} + \frac{k^+}{1 + \dfrac{K_{app}}{[H^+]}} \qquad (5)$$

where K_{app} is the apparent acid dissociation constant of amine and k and k^+ denote the real second-order rate constants of reductions by amine-free base (S) and conjugate acid (HS$^+$)

Table 1. Experimental Conjugate Acid Dissociation Constants, Redox Potentials, Second-Order Enzyme Reduction Rate Constants, and Apparent Conjugate Acid Dissociation Constants for Tertiary Amine Substrates **1**−**8** and Indoles **9** and **10**[a]

| substrate | pK_a[b] | E_{pa} (V)[c] | HRP compound I[d] | | HRP compound II[e] |
			k (M^{-1} s^{-1})	pK_{app}	k_1 (M^{-1} s^{-1})
1	9.60	0.54	4.7×10^5	9.7	1.0×10^4
2	9.59	0.55	1.2×10^5	9.8	2.2×10^3
3	9.22	0.74	2.5×10^4	9.5	2.0×10^2
4	9.18	0.66	1.8×10^4	9.5	1.5×10^2
5	9.12	0.70	1.3×10^3	9.1	14
6	9.19	0.72	3.0×10^2	9.2	24
7	9.21	0.89	9	9.3	$\sim$1.2[f]
8	9.39	0.79	69	9.3	7.1
9		1.26[g]	3.3×10^3		4.6×10^2
10		1.24[g]	2.83×10^{5} [h]		2.93×10^{4} [i]

[a] Derived rate constants of the free base forms of amines **1**−**8**. [b] Measured by potentiometric pH titration in 50% aqueous methanol. [c] Measured by cyclic voltammetry vs SCE: 3 mM substrates, 100 mM $NaClO_4$ in CH_3CN, glassy carbon, scan rate = 100 mV/sec. [d] The k and pK_{app} values are obtained from least-squares fits of pH-rate profiles according to eq 5. [e] The k_1 values were obtained from least-squares fits according to eq 6 for **9** or according to eq 7 for **1**−**8**. [f] Estimated using k_{app} at pH 9.00 according to eq 7. [g] From ref 18, vs SCE under slightly different conditions. [h] From ref 15. [i] Estimated from the k_{app} at pH 10.0 (ref 15) according to eq 6.
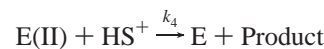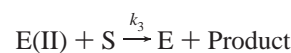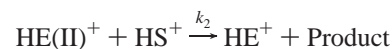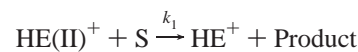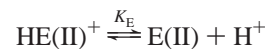
forms, respectively. Nonlinear least-squares fits of pH-rate profiles to eq 5 yielded apparent k^+ values that were both positive or negative but with absolute values that were at least 2 orders of magnitude smaller than k in all cases, suggesting that these values are experimental artifacts of the fitting routine, thus indicating that *reductions of compound I by the conjugate acid forms of amine substrates are negligible*. The pH-rate profiles were thus analyzed with the omission of the second term in eq 5 as exemplified with amines **1**−**8** in Figure 3. The real second-order rate constants (k) of the free base amine substrates and the apparent conjugate acid amine dissociation constants (pK_{app}) are listed in Table 1, along with the experimental pK_a values of these amine substrates measured in 50% aqueous methanol by potentiometric pH titration. The good agreement between calculated and experimentally determined pK_a values in MeOH−H_2O probably reflects at least in part that the operational dielectric of the enzyme active site is closer to 50% aqueous methanol than to pure water.

For compound II reactions, it is known that dissociation of the protonated distal His 42 affects the enzyme activity, with only the conjugate acid form presumably being active.[17] Indeed, the reduction rate of compound II by neutral compound **9** decreased with increasing pH in the range of pH 8−10. A nonlinear least-squares fit (Figure S3) according to eq 6 afforded the real second-order rate constant (k_1, Table 1), along with a pK_E value of 8.7, the same as the literature reported value.[17]

$$k_{app} = \frac{k_1}{1 + \dfrac{K_E}{[H^+]}} \quad (6)$$

For reduction of compound II by amine substrates **1**−**8**, one must take into account the ionization states of both enzyme and substrates. Theoretically, considering a possible low activity of the neutral His 42 form of compound II, four possible

(17) Dunford, H. B.; Adeniran, A. J. *Arch. Biochem. Biophys.* **1986**, *251*, 536−42.

combinations of enzyme and amine species contribute to the net reaction:

$$HE(II)^+ \underset{}{\overset{K_E}{\rightleftharpoons}} E(II) + H^+$$

$$HS^+ \underset{}{\overset{K_a}{\rightleftharpoons}} S + H^+$$

$$HE(II)^+ + S \xrightarrow{k_1} HE^+ + Product$$

$$HE(II)^+ + HS^+ \xrightarrow{k_2} HE^+ + Product$$

$$E(II) + S \xrightarrow{k_3} E + Product$$

$$E(II) + HS^+ \xrightarrow{k_4} E + Product$$

Rate constant k_4 represents reaction of compound II with amine substrate, both in their *inactive* forms (E(II) and HS^+), which is kinetically indistinguishable with k_1 and therefore can be omitted from the calculation. The kinetic expression of the apparent second-order rate constant is then deduced as

$$k_{app} = \frac{k_1}{\left(1 + \dfrac{[H^+]}{K_{app}}\right)\left(1 + \dfrac{K_E}{[H^+]}\right)} + \frac{k_2}{\left(1 + \dfrac{K_{app}}{[H^+]}\right)\left(1 + \dfrac{K_E}{[H^+]}\right)} + \frac{k_3}{\left(1 + \dfrac{[H^+]}{K_{app}}\right)\left(1 + \dfrac{[H^+]}{K_E}\right)} \quad (7)$$

where k_1 and k_2 represent the second-order rate constants for reactions of the protonated form of compound II with free base and conjugated acid forms of amine substrate, whereas k_3 is the second-order rate constant for reaction of the deprotonated form of compound II with the free base form of amine substrate. To simplify data analysis, all the nonlinear least-squares fits were conducted with the fixed pK_E value of 8.7 and pK_{app} values obtained from reductions of compound I by the same amines (Table 1), the most relevant set of operational pK_a values that would reflect actual variations in microenvironment. Analysis of pH-rate profiles according to eq 7 showed that k_3 is negligible for the most reactive **1**, whereas for the slowly oxidizing **2**−**4**, k_1, k_2, and k_3 all must be taken into account to achieve good fits, though k_1 is the major contributor in all cases (Supporting Information). By contrast, for cyclic benzylamines **5**, **6**, and **8**, k_2 and k_3 are both negligible, so that reduction of the protonated form of compound II by the free base amine form (k_1) is the only contributor. It should be noted that reduction of compound II by **7** was too slow to allow for construction of a pH profile. Assuming this reaction follows the same pH dependence as **5**, **6**, and **8**, k_1 for **7** was estimated from the k_{app} at pH 9.0 (0.13 M^{-1} s^{-1}) according to eq 7. Typical pH-rate profiles and nonlinear least-squares fits for compound II reductions are shown in Figure 4, and the rate constants k_1 are listed in Table 1. Values of k_2 and k_3 for **1**−**4** are listed in Table S1, along with a proposed rationale for these minor rate constants.

Metabolism. Following the determination of rates of oxidations of **1**−**4** by compounds I and II, we next verified that these more reactive substrates could be metabolized under turnover conditions. Since both the indole nucleus and the tertiary amine

Figure 3. The pH-rate profiles for reduction of compound I by cyclic 3-indoleethylamines **1**−**4** (left panel) and cyclic benzylamines **5**−**8** (right panel) and the corresponding nonlinear least-squares fit curves.
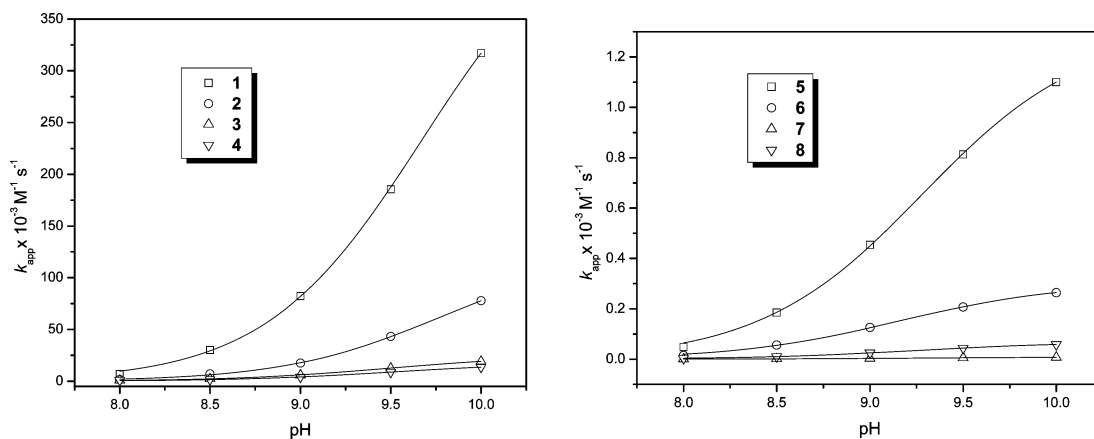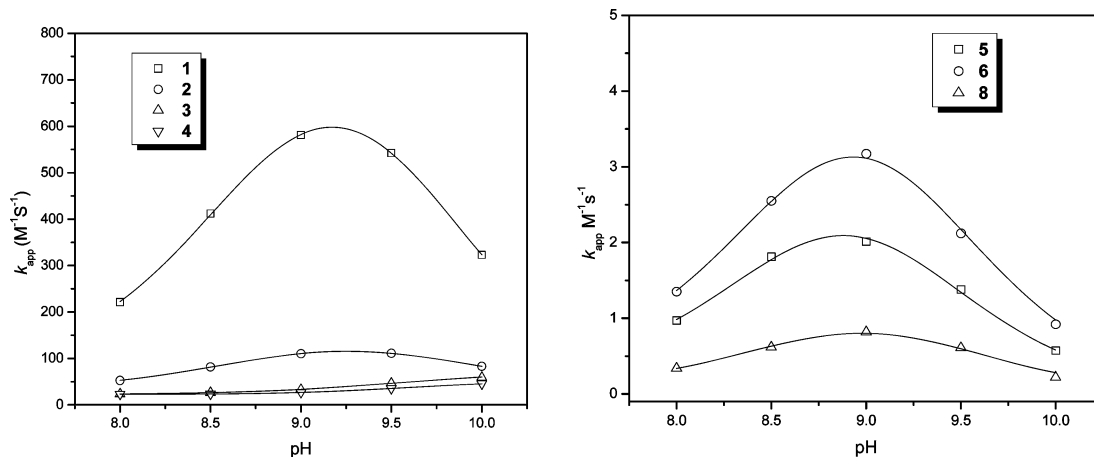

Figure 4. The pH-rate profiles for reductions of HRP compound II by cyclic 3-indoleethylamines **1**−**4** (left panel) and cyclic benzylamines **5**, **6**, and **8** (right panel) and the corresponding nonlinear least-squares fit curves.

moieties in **1**−**4** are susceptible to oxidation, it was expected that products reflecting both oxidation pathways would be found, and that such analysis could help deduce the *regiochemistry* of the operational initial 1e oxidations. To ensure that metabolism proceeds exclusively through the normal compound I/compound II catalytic cycle (excluding participation by compound III), a low ratio of H_2O_2/HRP was maintained in all reactions.[19]

Compound **2** was chosen for delineation of the metabolic profile (Scheme 2). Incubation of **2** (800 μM) with HRP (40 μM) and H_2O_2 (200 μM) in pH 8.0 phosphate buffer resulted in a fairly clean reaction mixture containing three major metabolites as assessed by reverse phase HPLC-UV detection at 290 nm (Figure 5). Fractions of each of these products were collected and subjected to MS analyses. On the basis of their ESI-MS and tandem MS fragmentation modes, the first and the second fast-eluting metabolites were assigned as 3-hydroxyindolenine **11** and aminoaldehyde/carbinolamine **12**/**13** (Scheme 2 and Supporting Information). The slow-eluting (less polar) metabolite had poor sensitivity to ESI-MS, but could be isolated in a preparative scale reaction and characterized as indole-3-

carboxaldehyde (**14**). The structure of **11** was confirmed by its ready conversion to authentic oxindole **15** upon heating with trifluoroacetic acid (Figure S6), a typical reaction of 3-hydroxy-indolenines.[20] The structure of **12**/**13** was confirmed by comparative HPLC and ESI-MS analyses with an authentic sample obtained by deprotection of the diBoc-protected aldehyde **16**, in turn obtained by DIBAL reduction of the ester **17** (Supporting Information).

The 3-hydroxyindolenine **11** represents the O_2-dependent indole oxidation (path A) previously observed in HRP oxidation of 3-alkylindoles, where cleavage products like **18** and oxindoles like **15** dominated (lower pH than in the current work).[15] The key intermediate for this pathway would be the hydroperoxide **19** formed following O_2 interception of the initially generated indole radical cation.[15] The absence of **18** in the present reaction is presumably due to the use of a high concentration of HRP such that the native HRP would quickly reduce any hydroperoxide **19** to **11**.[15] The ability of HRP to reduce organic hydroperoxides is well documented.[21] Product **12**/**13** is the hydrate form of the *endo*-iminum **21** generated following the initial amine oxidation (path B in Scheme 2). Amine oxidation

(18) Job, D.; Dunford, H. B. *Eur. J. Biochem.* **1976**, *66*, 607−14.
(19) (a) Silva, S. O.; Ximenes, V. F.; Catalani, L. H.; Campa, A. *Biochem. Biophys. Res. Commun.* **2000**, *279*, 657−62. (b) Ximenes, V. F.; Catalani, L. H.; Campa, A. *Biochem. Biophys. Res. Commun.* **2001**, *287*, 130−4. (c) Ximenes, V. F.; Campa, A.; Catalani, L. H. *Arch. Biochem. Biophys.* **2001**, *387*, 173−9.

(20) (a) Skordos, K. W.; Skiles, G. K.; Laycock, J. D.; Lanza, D. L.; Yost, G. S. *Chem. Res. Toxicol.* **1998**, *11*, 741−9. (b) Fennell, R. C. G.; Plant, S. G. P. *J. Chem. Soc.* **1932**, 2872−6.
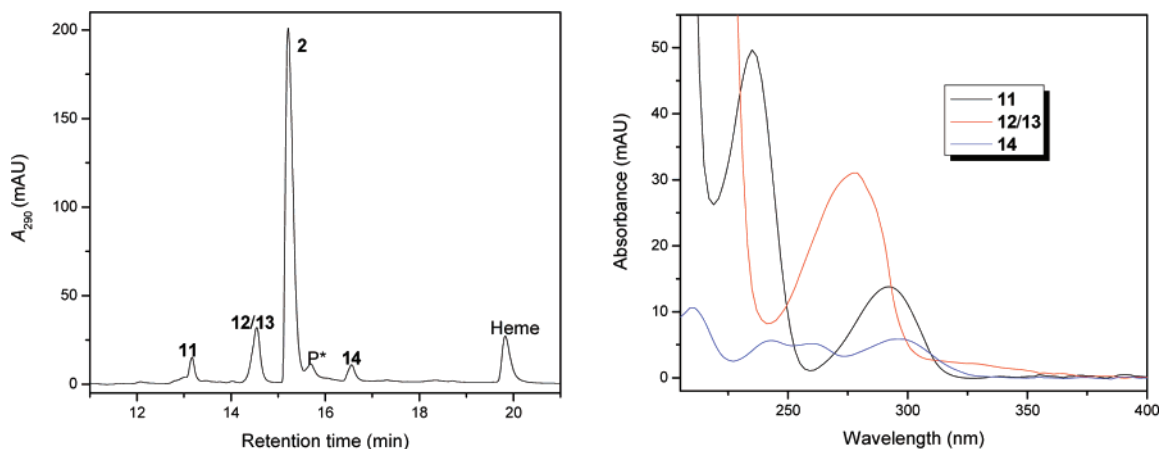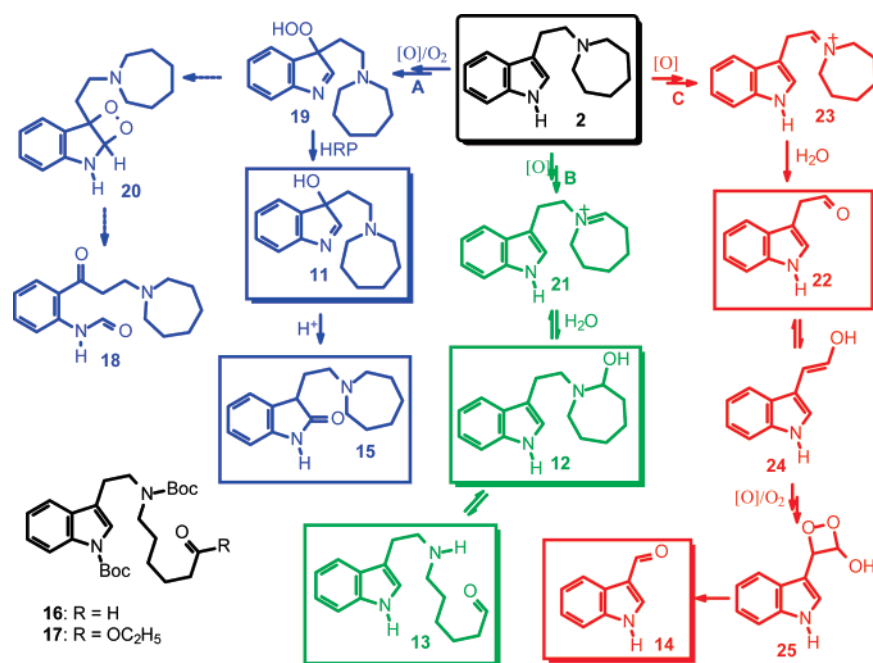
Figure 5. HPLC profile (290 nm) recorded upon 10 min incubation of HRP (40 μM), **2** (800 μM), and H_2O_2 (200 μM) in pH 8.0 phosphate buffer at 25 °C (left panel) and the corresponding diode array UV spectra of the major metabolites (right panel). During HPLC separation, HRP decomposes to protein (P*) and heme.

Scheme 2

would also be expected to generate *exo*-iminum **23**, likely to be the precursor of observed product **14**, through the intermediacy of indole-3-acetaldehyde (**22**) (path C). Indeed, there is an earlier report on HRP catalyzed oxidation of **22**, where up to a 50% yield of **14** could be observed at low pH.[22] The yield of **14** from **22** under our conditions was 45% by HPLC (Figure S7). Our finding of **14** rather than **22** in the HRP oxidation of **2** presumably reflects the fact that **22** was oxidized more rapidly than was the starting **2** by HRP/H_2O_2 in pH 8.0 phosphate buffer, thereby establishing **14** as an end product representing 45% of initial reaction along path C, Scheme 2. Although the mechanism of this formal skeletal truncation is unclear, evidence that the enol form **24** might be a key intermediate is that **22** underwent autoxidation, albeit slowly, to give **14** in pH 8 phosphate buffer

(Figure S7 and Supporting Information). On the basis of literature reports on electron-transfer oxygenation of enols,[23] one can postulate that oxidation of **24** to **14** involves formation and cleavage of a dioxetane intermediate **25**.

Under the same conditions, HRP oxidation of **1** or **4** also gave the corresponding amine oxidation products **14** and **29/32** or **31/34**, and indole oxidation products **26** or **28** (Figure S9). Surprisingly, HRP oxidation of **3** afforded only indole oxidation product **27**; no amine oxidation products **14** and **30/33** could be detected by HPLC (Figure S9). By comparison with HRP oxidation of **2**, the major metabolites in these reactions were tentatively identified by HPLC according to their diode array UV spectra and confirmed by ESI-MS according to their tandem MS fragmentation modes (Supporting Information). In particular, confirmation of the low yield metabolite **31/34** was aided by independent synthesis of an authentic sample, which was unstable and had to be generated *in situ* from diBoc-protected

(21) See for example: (a) Shirasaka, N.; Ohnishi, H.; Sato, K.; Miyamoto, R.; Terashita, T.; Yoshizumi, H. *J. Biosci. Bioeng.* **2005**, *100*, 653−6. (b) Adam, W.; Lazarus, M.; Hoch, U.; Korb, M. N.; Saha-Moeller, C. R.; Schreier, P. *J. Org. Chem.* **1998**, *63*, 6123−7. (c) Adam, W.; Hoch, U.; Lazarus, M.; Saha-Moeller, C. R.; Schreier, P. *J. Am. Chem. Soc.* **1995**, *117*, 11898−901.
(22) Yeh, R.; Hemphill, D., Jr.; Sell, H. M. *Biochemistry* **1970**, *9*, 4229−32.

(23) See for example, Wu, S.-P.; Liu, J.-F.; Jiang, Z.-Q. *Chem. Commun.* **1996**, 493−4.
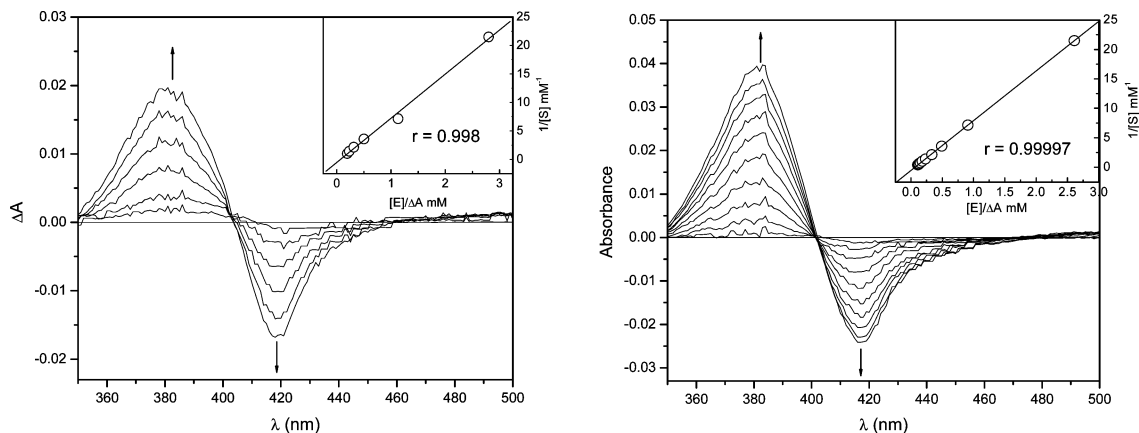
Figure 6. Difference spectra obtained by titration of native HRP (7.00 μM) with **2** (left panel) and **9** (right panel) in 0.1 M pH 10 borate buffer at 25 °C and the corresponding 1/[S] vs [E]/ΔA plots. Detailed conditions are given in the Experimental Section.

Table 2. Product Distributions in HRP Oxidations of **1**–**4**[a]

substrate	conversion[b] (%)	product distribution[c] (%)	% indole oxidation	% amine oxidation	amine oxidation endo:exo ratio
1	60	**26** (4.0), **29/32** (86.5), **14** (9.5)	4.0	96.0	9.1
2	35	**11** (29.0), **12/13** (60.7), **14** (10.3)	29.0	71.0	5.9
3	33	**27** (100)[d]	100	0	
4	12	**28** (86.4), **31/34** (11.7), **14** (1.9)	86.4	13.6	6.2

[a] All reactions were conducted in 0.1 M pH 8.0 phosphate buffer at 25 °C with an indole/ H_2O_2/ HRP ratio of 20:5:1. [b] Determined by HPLC after 10 min (after which there is no further reaction). [c] Normalized yields based on corrected HPLC integrals of the three major metabolites. The yield for **14** was corrected to reflect the % reaction along pathway C by dividing the observed yields of **14** by 45%, the observed yield of **14** obtained from a control HRP oxidation of **22** (see Supporting Information). [d] No amine oxidation products **30/33** and **14** were found by HPLC within the detection limit.

aldehyde **35** prepared by DIBAL reduction of ester **36** (Supporting Information). By normalizing the HPLC peak integrals of the three major metabolites, which were adjusted according to an estimation of their respective extinction coefficients at the same wavelength (Supporting Information), the relative product distributions could be estimated (Table 2), thereby allowing for an appreciation of the partitioning *not only between indole and amine oxidation pathways*, *but also between endocyclic and exocyclic amine oxidation pathways*.[24]

26: n = 3
27: n = 1
28: n= 0

29: n = 3
30: n = 1
31: n = 0

32: n = 3
33: n = 1
34: n = 0

35: R = H
36: R = OC$_2$H$_5$
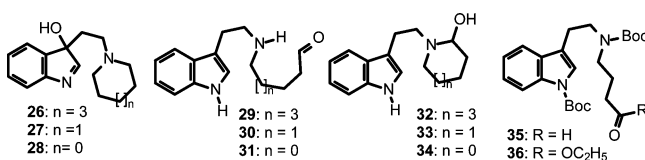
Assuming that only one-electron oxidation of substrates **1**–**4** by either compounds I or II is sufficient to result in final products (e.g., completion of reaction would be mediated by O_2), the limiting maximal conversions that could be obtained in the reactions reported in Table 2, based on the relative reactant stoichiometry used, were then 10% based on HRP (if no turnover) and 50% based on H_2O_2. Thus, in all cases, turnover is evident, and the conversion of **1** in excess of 50% must reflect at least some regeneration of HRP compound I by O_2-derived ROOH intermediates.

(24) If a large excess of H_2O_2 (2000-fold with respect to HRP) was used, the oxidations became rather complicated and the 3-hydroxyindolenines became the major products in all cases (see Figure S6 for an example). The reasons are that (1) all the major amine oxidation products can be further metabolized by HRP and (2), in the presence of a large excess of H_2O_2, compound III is the major oxidant, which has been shown especially capable of mediating indole oxygenation.[19]

Binding Affinities. Binding of substrates to native HRP was studied by optical difference spectroscopy.[8] In 0.1 M pH 7.00 phosphate buffer, preliminary experiments with **2** and **7** showed no detectable UV−vis difference spectral signals, suggesting that the binding affinity of the conjugate acid form of the aliphatic amines to HRP is low. Thus all the binding experiments were conducted at pH 10, as the best compromise between (i) ensuring high concentrations of the free base amine forms and (ii) preventing loss of enzyme activity at high pH. Typical difference spectra of complexes of native HRP with **2** and **9** are shown in Figure 6, and those with **7** are shown in Figure S3. Analysis of these spectra (Experimental Section) yielded the molar absorptivity differences $\Delta\epsilon$ of the free and bound enzyme and the apparent dissociation constants K_d^{app}, which were then converted to K_d values for the amine free base forms (Table 3).

Two distinct spectral patterns were observed: (1) λ_{max} and λ_{min} at 380−383 and 417−420 nm, respectively, and isosbestic points at 399−406 nm, seen for **1**–**4**, **9**, and **10**, and (2) λ_{max} and λ_{min} at ca. 402 and 420−423 nm, respectively, and isosbestic point at ca. 413 nm, seen for **5**–**8**. Although data could not be obtained in some cases because of solubility problems, it is clear that the binding affinities of the substrates are similar. Under the same conditions, no UV−vis difference spectral signals could be detected with *N*-methyl cyclic amines (Supporting Information), indicating probable nonbinding of simple aliphatic amines lacking an aryl substituent.

Kinetic Saturation. Confirmation that observed binding of amine substrates to native HRP provides reasonable evidence that electron-transfer to compounds I and II occurs via similar enzyme−substrate association complexes, requires a demonstra-
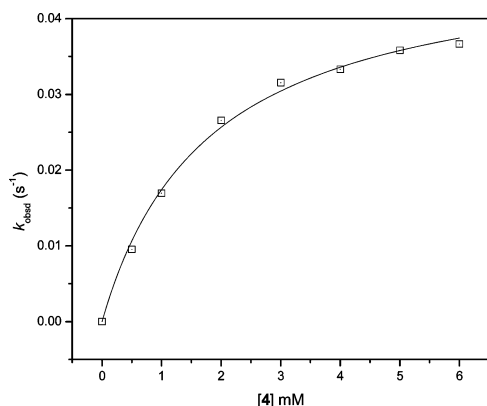
Figure 7. Plot of pseudo-first-order rate constant (k_{obsd}) vs substrate concentration obtained in reduction of HRP compound II (21 μM) by **4** in 0.1 M of pH 9.00 phosphate buffer at 25 °C and the corresponding nonlinear least-squares fit according to eq 3.

Table 3. Difference Spectral Parameters and Dissociation Constants of HRP-substrate Complexes[a]

substrate	λ_{max} (nm)	λ_{min} (nm)	isosbestic point (nm)	K_d^{app} (mM)	$\Delta\epsilon_{peak\sim trough}$ (mM^{-1} cm^{-1})	K_d (mM)[c]
1[b]	381	418	404			
2	380	418	404	1.9	15	1.4
3	381	418	405	1.0	10	0.72
4	381	418	405	1.0	12	0.86
5[b]	402	423	413			
6[b]	402	423	413			
7	402	423	413	1.3	3.3	1.1
8	402	423	413	1.8	2.0	1.4
9	383	417	402	1.9	16	
10	382	418	399	0.90	13	

[a] Data obtained in 0.1 M pH 10 borate buffer at 25 °C. [b] Because of poor solubility of substrate the peak and trough could be seen only at low concentrations, no reasonable data analysis could be achieved. [c] Dissociation constants of the free base amine forms.

tion that the kinetics of substrate oxidation follows a saturation phenomenon predicted by the preassociation equilibrium defined in eq 3; that is, the k_{obsd} should plateau at high substrate concentrations. In practice, saturation for enzymes like HRP is rarely observed because (i) most aromatic substrates of HRP possess K_d values in the millimolar range and (ii) these substrates are usually poorly soluble, confounding obtaining kinetic data at high substrate concentration. Nonetheless, rate data for compound II reduction by **4** could be obtained at high concentration for this fortuitously more soluble substrate. Although the maximum plateau rate was not reached experimentally, the k_{obsd} versus [**4**] plot clearly exhibits saturation behavior (Figure 7).

A nonlinear least-squares fit of this plot according to eq 3 afforded a K_d^{app} value of 1.79 ± 0.16 mM, and a k_{cat} value of 0.0486 ± 0.0015 s^{-1}, indicating that the highest concentration of **4** used (6 mM) attained ~80% saturation. According to eq 4, the k_{app} can be calculated as 27.2 s^{-1} M^{-1}, which matches well with the k_{app} (27.0 s^{-1} M^{-1}) obtained at the same pH using a low concentration of **4** (Figure 2). Moreover, correcting the kinetically determined K_d^{app} value by the amine pK_a yields an estimate of the binding constant K_d of **4** free base with HRP compound II as 0.71 mM, which is close to the binding constant of **4** free base with native HRP (0.86 mM) measured by optical difference spectroscopy (Table 3). We can extrapolate this finding and conclude that the remaining K_d values listed in Table

3 are reasonable estimates for binding affinities of substrates to the oxidative forms of HRP. These results are important (i) in that this is one of the first examples of kinetic saturation behavior seen for HRP[25] and (ii) in that because $k_{app} = k_{cat}/K_d^{app}$ (eq 4); despite the low binding affinities, we can conclude that substrate binding contributes directly to the apparent second-order rate constants.

Binding Mode. To investigate the basis of the experimentally determined K_d values for the cyclic tertiary amine free base forms with native HRP, possible binding modes of **1**−**8** were examined by computational docking simulation, starting with the published crystal structure of the enzyme and the energy-minimized conformation of each amine. Docking modes to the active site energy grid were investigated using the Discovery Studio Software Package PC Version 1.7, which examines possible rotation about each single bond in the substrate and then allows assignment of energy scores according to the newly developed scoring function LigScore2.[26]

Crystallographic studies have shown that the conformations of native HRP and compounds I and II are almost identical;[27] thus we relied on the coordinates of the native enzyme to shed light on structural features that might determine both compound I and II oxidation rates. Of all the docking modes defined by the program (14−22 modes for **1**−**4**, and 8−9 modes for **5**−**8**), >95% of them involve orientation of the ligand molecules with the aromatic rings pointing toward the heme edge and the azacycles projecting out of the heme pocket (Figure S14). On the basis of this statistical preference and the well-known ability of simple aromatics (e.g., phenols and anilines) to bind to the "heme edge" binding domain, as well as a recent computational docking study of serotonin and melatonin with HRP,[28] we propose that *substrates **1**−**8** all bind to the enzyme through their aromatic nuclei*.

For both *N*-(indole-3-ethyl) and *N*-benzyl series of substrates, two universal and leading scored docking modes (DM I and II) were identified (Figures 8 and S15). These two modes differed in terms of the distance between substrate aromatic ring and the heme edge, though the positioning of the azacycle was nearly overlapping. Thus, whereas the amine nitrogen−heme distances in both modes are 9−11 Å for all substrates, the minimum aromatic terminus−heme distances in DM I are longer for **5**−**8** (5.5−6.5 Å) than for **1**−**4** (4−5 Å), and are even longer (7−8 Å) in DM II for all substrates (Table S6).

For the *N*-(indole-3-ethyl) series **1**−**4**, although ancillary van der Waals and/or hydrophobic interactions between the substrate indole ring and three aromatic residues (Phe-143, Phe-142, and Phe-179) appear to be involved in both modes, the major distinguishing feature of DM−I is an apparent stabilizing interaction of the indole ring with the heme, whereas in DM II, the major stabilizing interaction appears to be with Phe-68. In the case of the *N*-benzyl series **5**−**8**, whereas docking simulations again resulted in two principal docking modes, the distinction between the two modes is more subtle, reflecting

(25) For one example of kinetic saturation for HRP compound II reduction by *p*-cresol see: Critchlow, J. E.; Dunford, H. B. *J. Biol. Chem.* **1972**, *247*, 3703−13.
(26) Krammer, A.; Kirchhoff, P. D.; Jiang, X.; Venkatachalam, C. M.; Waldman, M. *J. Mol. Graphics Modell.* **2005**, *23*, 395−407.
(27) Berglund, G. I.; Carlsson, G. H.; Smith, A. T.; Szoke, H.; Henriksen, A.; Hajdu, J. *Nature* **2002**, *417*, 463−8.
(28) Hallingback, H. R.; Gabdoulline, R. R.; Wade, R. C. *Biochemistry* **2006**, *45*, 2940−50.
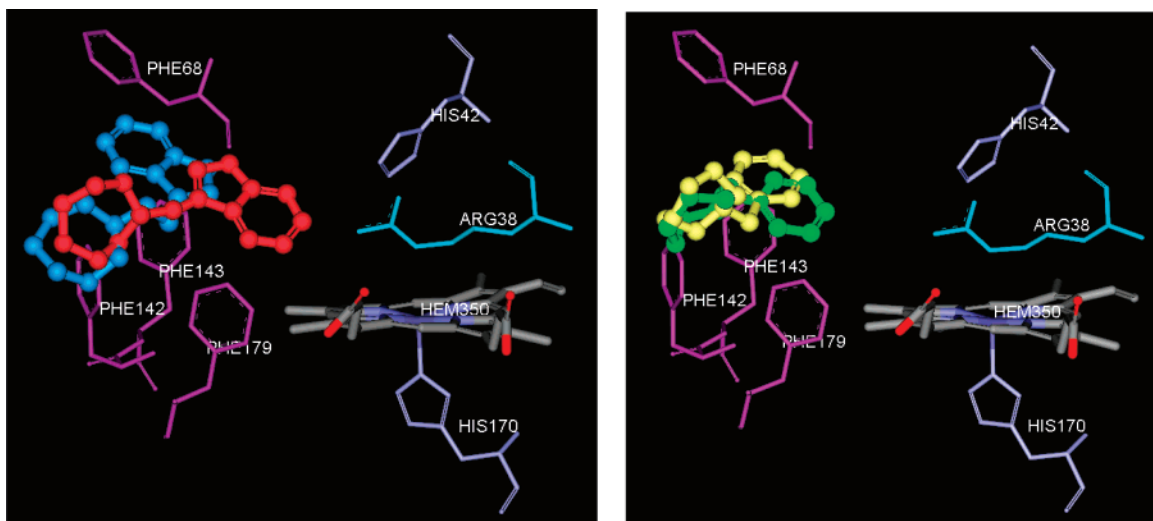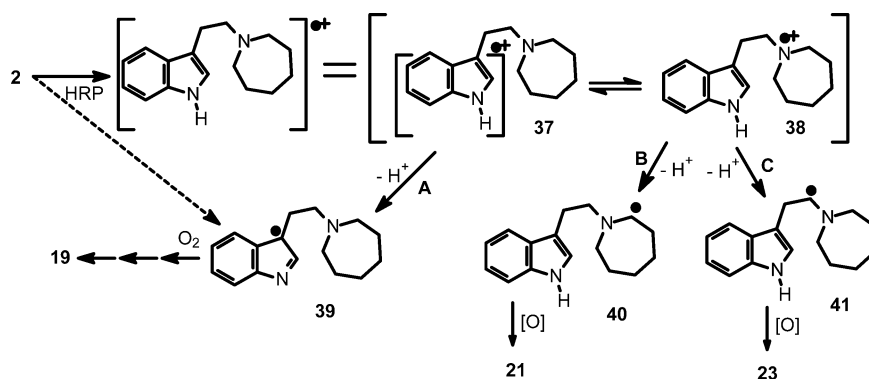
Figure 8. Best scored docking modes for **2** (left panel, DM I (red) and DM II (blue)) and **6** (right panel, DM I (green) and DM II (yellow)). The mouth rim of HRP heme pocket is defined by four hydrophobic residues: Phe-143, Phe-142, Phe-179, and Phe-68.

Scheme 3

differences in the orientation of the phenyl ring relative to the Phe residues lining the mouth of the "heme edge". Thus, if it is assumed that the main operational binding mode in both substrate series is defined by DM−I, where the substrate aryl ring is closer to the heme edge, then the better heme proximity of the indole ring in **1**−**4** than of the phenyl ring in **5**−**8** may explain the distinct optical difference spectra and larger extinction coefficients with HRP observed for amines **1**−**4** (and indoles **9** and **10**) relative to those for amines **5**−**8** (Table 3).

Discussion

Structure−Reactivity and Mechanism. Previous studies have established that simple aliphatic tertiary amines are poor substrates of HRP under turnover conditions.[13] Here we confirmed that reductions of HRP compounds I and II by *N*-benzyl cyclic amines **5**−**8** are slow (Table 1) and nearly as slow as are the reductions by the corresponding *N*-methyl cyclic amines (Table S4). In contrast, reductions of compounds I and II by *N*-(indole-3-ethyl) cyclic amines **1**−**4** are 2−3 orders of magnitude faster (Table 1), and preparative turnover reactions could be observed, especially in the case of amine **1**. Given that indole (**9**) and especially 3-methylindole (**10**) also react with HRP fairly quickly (Table 1), the fast reductions by **1**−**4** could simply reflect reactions with the indole nucleus in these compounds. However, a full product analysis of HRP metabo-

lism of **1**−**4** revealed that except for **3** (affording strictly indole oxidation products), reactions of the five-, seven-, and eight-membered azacycle compounds led to a mixture of indole and amine oxidation products, with the latter predominating in the case of **1** and **2** (Table 2). The product study also revealed that *endo*cyclic amine oxidation predominated over *exo*cyclic amine oxidation (Table 2), consistent with five-, seven-, and eight-membered rings favoring an *endo*cyclic rather than *exo*cyclic double bond.

When one examines the product distribution data reported in Table 2, it is seen that the faster rates for compounds **1** and **2** (Table 1) correspond to those cases where there is more product deriving from amine rather than indole oxidation. Because k and k_1 for oxidations by compounds I and II, respectively, were measured using large excesses of substrates at the initial stage of conversion, it is reasonable to assume that these rates represent initial one-electron oxidations to generate radical cations that would not compete with the starting substrates in reducing compounds I and II. The radical cations (shown for **2** in Scheme 3) would subsequently partition among various possible pathways for loss of proton, ultimately reflecting paths A−C described in Scheme 2.

For indoleethylamines **1**−**4**, we suggest that there are two high-lying filled molecular orbitals (MOs), one with the largest coefficients in the indole π system and one with the largest
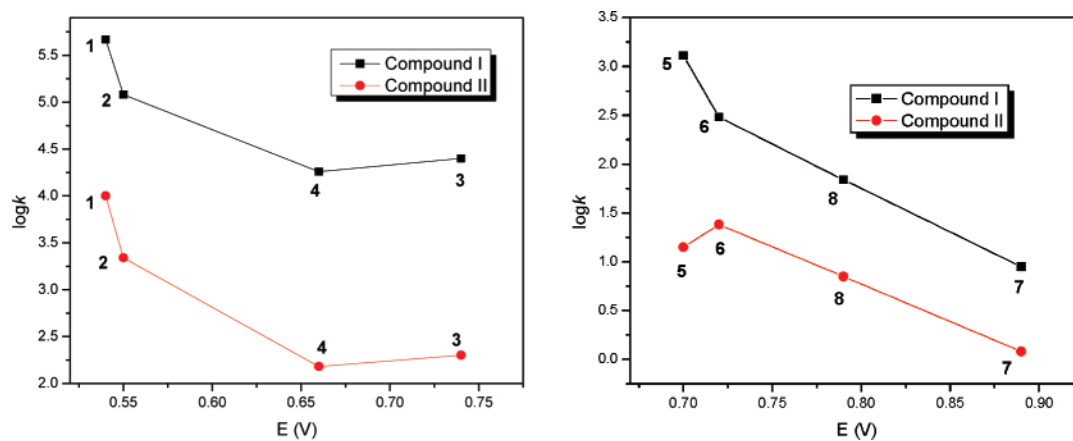
Figure 9. Linear free energy plots correlating the oxidation rates of cyclic 3-indoleethylamines **1**−**4** (left panel) and cyclic benzylamines **5**−**8** (right panel) with redox potentials.

coefficients on the amine nitrogen lone pair. Thus, one electron oxidation would result in two rapidly equilibrating valence tautomeric radical cations, one where the half-filled orbital density is distributed mainly on the indole ring (electronic state **37**) and the other where it is distributed mainly on the tertiary amine nitrogen (electronic state **38**). Product partitioning would then reflect the position of this equilibrium, governed by the relative energy of these two MOs, in turn reflecting redox potentials and the conformations of the substrate amines bound to HRP.

It is well-known that the rates of chemical (e.g., $K_3Fe(CN)_6$[12a] or Cu(II)[29]) or electrochemical[12b,12c] oxidation of cyclic amines depend critically on ring size, since the rehybridization from sp^3 to sp^2 that occurs upon one-electron oxidation is conformationally favored by five-, seven-, and eight-membered rings but disfavored by six-membered rings on the basis of torsional strain factors. Our observed electrochemical E trend (for both series of compounds) $8 \leq 7 < 5 < 6$ is congruent with the E trend observed for the corresponding N-methyl cyclic amines.[12c] Thus, the faster rates of oxidation of **1** and **2** reflect favorable one-electron oxidations of the tertiary amine centers in the seven- and eight-membered azacycles, associated with the relatively greater stabilizing nature of aminium radical cation forms like **38** for these ring sizes. In contrast, the less favorable one-electron oxidation of the tertiary amine center in the six-membered ring substrate **3** reduces the importance of **38** for this ring size, in turn manifesting in exclusive indole oxidation. Since compounds I and II were shown to have similar regioselectivity in oxidizing a selected cyclic 3-indoleethylamine substrate (Supporting Information), the conclusions above appear to pertain to both sets of rate constants listed in Table 1.

Linear Free-Energy Relationships. For a structurally related series of compounds such as **1**−**4** or **5**−**8**, one might expect to witness a linear free-energy relationship (LFER) between rates and thermodynamic parameters, as is seen for rates of HRP oxidation of substituted phenols and anilines as a function of Hammett substituent constants σ.[18] When the process involves electron-transfer and the thermodynamic property is redox potential, it has been more common recently to discuss rate trends according to Marcus theory. The advantage of the latter over a simple LFER treatment is that the Marcus equation explains the leveling off of rates as they increase to the point

where the process becomes thermodynamically activationless. Our rates, however, are in the slower linear range of typical Marcus plots. The absence of data in the fast regime prevents a quantitative analysis according the Marcus equation, which requires a curved plot to solve for the two unknown parameters (the reorganization energy and the activationless rate).[30]

For our mechanistic needs, where it is assumed that the electron-transfer distance is the same within each series of amines, simple plots of log k vs E are more suitable,[31] and are shown in Figure 9 for the cyclic voltammetry data. Although the plots for compounds **5**−**8** are roughly linear (there are only four experimental points, so a statistical analysis of linearity seems unwise), the plots for compounds **1**−**4** are markedly curved. The leveling out of plots in going from compounds **1**, **2**, **4** to compound **3** correlates with the point where the oxidation product profile changes from one reflecting a mixture of indole and amine oxidation to one reflecting strictly indole oxidation. Our interpretation is that whereas HRP-mediated oxidations of **5**−**8** involve strictly one-electron oxidations of the tertiary amine center, oxidation rates for the indoleethylamines reflect a changeover from mainly amine oxidation for low potential amine centers, ultimately to mainly indole ring oxidation when the amine potential becomes sufficiently high.[32] Indeed, such a change in mechanism would predict a curved LFER plot. As an academic exercise, one could attempt to treat the partitioning shown in Scheme 3 by partitioning the measured k values into two components (amine oxidation vs indole oxidation) on the basis of product yield distribution. The expectation would be that the k_{indole} values would be relatively constant and that the k_{amine} values would exhibit a more linear free-energy dependence on electrochemical potential. Our data appear to support this expectation (Supporting Information).

How Does the Auxiliary Indole Ring Promote Amine Oxidation? If the low reactivity toward HRP of simple aliphatic amines (e.g., cyclic methylamines, Supporting Information) is partly due to lack of binding, then the significantly improved

(29) Wang, F.; Sayre, L. M. *J. Am. Chem. Soc.* **1992**, *114*, 248−55.

(30) Folkes, L. K.; Candeias, L. P. *FEBS Lett.* **1997**, *412*, 305−8.
(31) Colosi, L. M.; Huang, Q.; Weber, W. J., Jr. *J. Am. Chem. Soc.* **2006**, *128*, 4041−7.
(32) On the basis of the voltametrically measured redox potentials of **1**−**4** (Table 1) relative to the higher values of typical 3-alkylindoles (Waltman, R. J.; Diaz, A. F.; Bargon, J. *J. Phys. Chem.* **1984**, *88*, 4343−6), it might be predicted that oxidations of all four indoleethylamines would lead strictly to amine oxidation products. However, oxidation outcome also reflects the fact that it is the indole ring that is bound at the heme edge and is thus closest to the HRP oxidants.

binding affinity of **1–4** and **5–8** would explain their enhanced reactivity. Indoleethylamines **1–4** have lower potential and react faster. However, although binding of these compounds occurs through the indole ring, in three of the four cases, the product mixtures derive partly or mainly from oxidation at the tertiary amine center. It thus appears that binding of the indole ring leads to substrate-HRP complexes that are conformationally disposed for mediation of what effectively becomes medium long-range SET oxidation of the tertiary amine centers by the active oxidants of compounds I and II.

We are aware of recent studies suggesting that oxidation of phenolic substrates by HRP involves a *proton-coupled* electron-transfer (PCET) process, and that the involvement of an porphyrin radical cation isomer of compound II (P$^{+\bullet}$Fe(III)-OH rather than PFe(IV)-OH) would permit a convergence of PCET details for both compound I and II reductions.[33] Although PCET would not apply to the oxidation of tertiary amine to tertiary aminium radical cation, oxidations by HRP leading to indole oxidation products could well be facilitated by a PCET process, leading directly to neutral indolin-3-yl radicals like **39** (hashed arrow in Scheme 3).

Conclusion

Despite the recognition in some circles that aliphatic (as opposed to aromatic) amines are poor substrates for HRP, this realization has not been elaborated in the literature. To our knowledge, the current study is the first to address this problem systematically, and to identify one case that meets the criteria needed for observing reaction. Thus, indoleethylamines that contain tertiary amine centers that are unusually susceptible to one-electron oxidation (due to geometrically enforced hybridization factors) are excellent substrates for HRP and can undergo turnover. It appears that the electron-rich indole ring not only improves binding but, more importantly, is also able to mediate the electron transfer between the tethered tertiary amine center and the HRP oxidant centers. The latter factor is undoubtedly under conformational control, and the successful oxidation of Vinca alkaloids by HRP[14] may further reflect the enforcement, by the rigid ring system, of an appropriate orientation of the tertiary amine lone pair relative to the indole ring. It is proposed that although the indole ring is needed to "anchor" the alkaloid molecule at the heme crevice, the lowest energy electron transfer generates a radical cation localized mainly on the tertiary amine nitrogen rather than indole ring.

On a broader perspective, our results confirm that a key determinant of substrate activity for HRP is the availability of a flat and rigid aromatic domain that can appropriately fit the heme crevice. In this regard, although the physiological relevance of aliphatic amine oxidation by peroxidases is unclear, the ability of a redox-active aromatic moiety to facilitate oxidation of an aliphatic electron donor may be important in drug development and xenobiotic metabolism.

Experimental Section

General experimental methods, synthesis and characterization of amine substrates, determination of acid dissociation constants, and details of product characterization for HRP oxidations, including preparative oxidations, appear in Supporting Information.

(33) Derat, E.; Shaik, S. *J. Am. Chem. Soc.* **2006**, *128*, 13940–9.

Kinetics of Reductions of HRP Compounds I and II by 1–9. HRP compound I was freshly prepared each time by mixing 3 mL of HRP stock solution in buffer with a 10-fold excess of H$_2$O$_2$ in a 3-mL quartz cuvette, to which was quickly added an appropriate amount of substrate.[15] The reaction was immediately followed by monitoring the appearance of the compound II Soret band (419 nm for pH 8 and 420 nm for pH 9 and 10), and the data were then analyzed using Origin 7.5 (Figure 1). The substrate concentration (excess) was chosen so that the rate in the presence of substrate was more than 10 times faster than the background enzyme decay rate measured in the absence of substrate. A fresh solution of compound II was prepared each time by the addition of 1 equiv of H$_2$O$_2$ to the native HRP solution (3 mL, 2.1 μM in buffer) and then waiting for 45 min.[15] After the addition of at least 10-fold excess of substrate to the cuvette containing compound II, the reaction was followed by monitoring the appearance of the native HRP Soret band at 403 nm, and the data were analyzed using Origin 7.5 (Figure 2). The background decay of compound II was very slow and could be neglected. Control experiments showed that the substrates were all stable in buffer. Blank cuvets in these experiments contained only the appropriate buffer.

Binding Experiments. Difference spectra (enzyme–substrate complex vs enzyme) were recorded in the following manner using solutions of **1–8** that were each pre-equilibrated to 25.0 °C. Initially, both the sample and reference cuvets were filled with 3 mL of the HRP solution (7 μM in buffer). Then small volumes of the substrate solution were successively added to the sample cuvette, with concomitant addition of the same volume of buffer into the reference cuvette. After each addition, the contents of both cuvets were mixed well, and the difference spectrum was recorded. In the meantime, the absorption spectra of substrates at all the operational concentrations were also recorded using similar procedures in the absence of HRP. All the difference spectra were corrected by deduction of both the baseline and the corresponding substrate absorption spectra using Origin 7.5 software. Volumes of standard HRP and substrate stock solutions were mixed to attain 10 different final solutions with [HRP] ranging from 7.00 to 6.75 μM and the [substrate] ranging from 0 to 2.04 mM. In some cases, severe precipitation occurred during the titration and only the spectra for solutions that remained homogeneous were used in the calculations (Figures 6 and S11).

From the difference spectra, the apparent dissociation constants K_d^{app}, and the molar absorptivity differences $\Delta\epsilon$ of the free and bound enzyme were obtained[8] from a plot of 1/[S] vs [E]/ΔA according to

$$\frac{1}{[S]} = \frac{\Delta\epsilon[E]}{K_d^{app}\Delta A} - \frac{1}{K_d^{app}}$$

For amine substrates, the binding of conjugate acid forms were neglected, and the binding constants K_d of free base were estimated according to

$$K_d = \frac{K_d^{app}}{1 + \dfrac{[H^+]}{K_a}}$$

Kinetic Saturation Phenomenon. A stock solution of **4** (40 mM) was prepared by first dissolving the HCl salt form of **4** in water, and then titrating the solution with aqueous NaOH to pH 8.2 (higher pH resulted in precipitation). This was found adequate to permit dilution into pH 9 buffer without causing a significant pH change (<0.02). To a 3-mL quartz cuvette were added 21 μM of HRP and a prescribed volume of 0.1 M of pH 9.00 borate buffer. After mixing, 21 μM of H$_2$O$_2$ was added, and the mixture was allowed to stand at 25 °C for 45 min to give HRP compound II. Then a prescribed volume of the 40 mM stock solution of **4** was added to achieve a final volume of 3 mL. After rapid mixing, the reaction was monitored at 403 nm at 25 °C.

The collected data were analyzed as above to give the observed pseudo-first-order rate constants k_{obsd}, which were then plotted against substrate concentrations (Figure 7). A nonlinear least-squares fit of the plot according to eq 3 was conducted using Origin 7.5 to yield k_{cat} and K_d^{app}.

General Procedures for HPLC and ESI-MS Analyses of HRP Oxidations of Indoleethylamines. To a solution of an indoleethylamine substrate (**1**−**4**, 800 μM) and HRP (40 μM) in 0.1 M pH 8.0 phosphate buffer (100 μL) was added 2 μL of 10 mM of aqueous H_2O_2 at 25 °C. After quick mixing, the brown solution immediately turned green, then red, and finally brown. A 20 μL aliquot of the reaction mixture was taken at the 10 min point and analyzed by HPLC using a 4.6 mm × 250 mm Agilent SB C18, 5 μm column, a flow rate of 1 mL/min, and a gradient mobile phase composed of HPLC-grade solvents A (5% aqueous CH_3CN) and B (95% aqueous CH_3CN), both containing 0.2% (v/v) TFA, according to the following program: 100% A to 95% A 0−20 min, 95% A to 100% A 20−25 min. Addition of another 2 μL H_2O_2 to the reaction mixture again resulted in an immediate color change to green, then to red, and finally to brown, indicating that only the normal compound I/compound II catalytic cycle was involved.

For ESI-MS analysis, the above incubation was repeated, but with HRP, indoleethylamine substrate, and H_2O_2 all being 5-fold more concentrated. After incubation for 20 min, the reaction mixture was subjected to HPLC separation using the same conditions as above. The fractions containing the major metabolites were collected and subjected to ESI-MS and tandem MS analysis on a ThermoFinnigan LCQ Advantage instrument operating in the positive mode using nitrogen as auxiliary gas. The instrument was set in the syringe pump mode, with the heated capillary temperature being maintained at 100−150 °C. The source voltage was 4.57 kV and the capillary voltage was 8.27 V.

Docking Simulation. Ligand structure construction and energy minimization were performed on the Chem3D Pro 10.0 platform of the ChemOffice software package (Cambridge). Only the free base form of amine substrates was considered. In constructing the ligand models, the conformations of azacycles were first optimized by MM2 and then attached to the indoleethyl or benzyl groups in an equatorial manner, and the resulting conformations were further energy minimized. For **5**−**8**, only two bonds are rotatable, and the most stable conformation can be readily determined. For **1**−**4**, however, three bonds are rotatable.

A full conformational analysis for **3** was thus conducted and the energies of various conformations were minimized by ab initio calculation using Gaussian 03 to figure out the most stable one (Supporting Information). All other congeners (**1**, **2**, and **4**) were then assigned the same conformations as **3**, which were energy minimized with MM2.

The crystal structure (PDB format) of native HRP (1H58)[27] in the Protein Data Bank was loaded on the Accelrys Discovery Studio software package (PC version 1.6). All the crystal water molecules were removed, and hydrogens were added by the program. The bond grades of the heme residue and charges on the heme oxygen, the heme iron, and its coordinating nitrogens were corrected manually. Protonation states of all other ionizable amino acid residues were set as default. The active site was then identified, and the energy grid was set automatically by the program. The energy minimized; most stable ligand structures (MOL format) were loaded. The "energy grid forcefield" was set as "Drieding", the "conformation search number of Monte Carlo trials" was set as 30000, and "pose saving perform clustering" was allowed, with "pose saving maximum cluster per molecule" being set as 100. Each output pose represents the energy minimum of a cluster of poses and is thus considered as a docking mode. The "scoring scores" option was set as LigScore2. Other parameters were set as default. After calculation, the output poses were ranked according to the LigScore2 scores, visualized, and analyzed. The results are shown in Figures 8, S14, and S15 and Table S6.

Supporting Information Available: Figures S1−S16, Tables S1−S7, determination of minor rate constants for compound II reduction, ESI-MS characterization of HRP metabolites of **1**−**4**, validation of determining product distributions by HPLC, HRP oxidations and binding of cyclic *N*-methylamines, ab initio calculations to determine the most stable conformation of **3**, partitioning rate constants for oxidation of **1**−**4** into k_{indole} vs k_{amine} components, and detailed experimental methods. This material is available free of charge via the Internet at http://pubs.acs.org.

JA075905S